Computational Materials Science 79 (2013) 599–610

Contents lists available at SciVerse ScienceDirect

Computational Materials Science

journal homepage: www.elsevier.com/locate/commatsci

Evolution of the electronic structure and properties of charged titanium doped aluminum nanoclusters

Yusuf Erdogdu [a], Şakir Erkoç [b,*]

[a] Department of Physics, Ahi Evran University, 40100 Kirsehir, Turkey
[b] Department of Physics, Middle East Technical University, 06800 Ankara, Turkey

ARTICLE INFO

Article history:
Received 10 December 2012
Received in revised form 1 July 2013
Accepted 5 July 2013
Available online 7 August 2013

Keywords:
Charged aluminum clusters
Titanium doping
DFT calculations
Relative energy
Structural stability
Electron affinities and ionization potential

ABSTRACT

A systematic study of the titanium doped aluminum clusters with various spin multiplicities have been performed by using Density Functional Theory calculations at the B3LYP/6-311++G(d,p) level. The HOMO–LUMO energy gap, ionization potential (IP), electron affinity (EA), Adiabatic Electron Affinity (AEA), Vertical Electron Affinity (VDE) and vertical detachment energy (VDE) are also computed for the most stable isomer of each cluster.

1. Introduction

Investigations of the geometries, electronic structures, energetic and reactivities of atomic clusters have attracted significant interest in recent years. One of the principal goals of these research activities is to explore the size evolutionary patterns of the properties of material aggregates from the molecular to condensed phase regime. Clusters play an important role in understanding the transition from microscopic to macroscopic structures of matter [1]. Thus, by studying the properties of clusters as a function of size, one hopes to learn how the bulk properties evolve. During the last few years, studies of transition metal clusters have attracted a lot of interests. In addition to, atomic clusters may have unique size specific properties that differ from their bulk systems. Consequently, materials synthesized by assembling clusters may be technologically important.

Among the group III elements aluminum, gallium and indium are the favorite metallic elements for cluster studies. Aluminum is a very common metal and has found many uses in everyday life. Small clusters composed of aluminum atom have naturally been the subjects of intensive studies for the last two decades. A large number of studies of aluminum cluster; both theoretical [3,15–19] as well as experimental [2–13] have been reported. In recent years, a number of series of experimental and theoretical works have been performed to study the structure, energetic stability, ionization potentials (IP), and electron affinities (EA) of the gas-phase elemental Al_n [14,3,16–17] and doped aluminum clusters AlnC [18], AlnSi [19], AlnP [20], AlnZn [21], AlnCr [22], AlnMn [22], AlnFe [22], AlnCo [22], AlnNi [22] and AlnBe [23] n varying from 2 to 23, and also the family of icosahedral XAl12 clusters with inserted heteroatoms X from the third and fourth main groups [24]. In addition, the dissociative chemisorption of molecular hydrogen on charged and neutral aluminum clusters $Al_{12}X$ (X = Mg, Al, Si) was investigated using DFT by Henry et al. [25]. Henry et al. [26] reported that the structure and bonding in charged and doped aluminum clusters have been investigated using Regional Density Functional Theory (RDFT). The structural electronic and other properties of the XAl12 type clusters was performed by Charkin et al. [27–29].

In this work, DFT-B3LYP at 6-311++G(d,p) [30,31] level is employed via the Gaussian 09 program [32] to optimize the structures of the Al_n (±) and $Al_{n-1}Ti$ (±) ($n \leqslant 7$) clusters. The analysis of the energetic and structural stability of these clusters depends on the various isomers that are presented. The HOMO–LUMO energy gaps, vertical detachment energy, vertical and Adiabatic Electron Affinity and adiabatic ionization potentials have been determined.

2. Method of calculation

The lowest-energy geometries of charged pure and the titanium doped aluminum clusters in the range of 1–7 derived from

* Corresponding author. Tel.: +90 312 2103285; fax:+90 312 2105099
E-mail address: erkoc@metu.edu.tr (Ş. Erkoç).

0927-0256/$ - see front matter © 2013 Elsevier B.V. All rights reserved.
http://dx.doi.org/10.1016/j.commatsci.2013.07.010

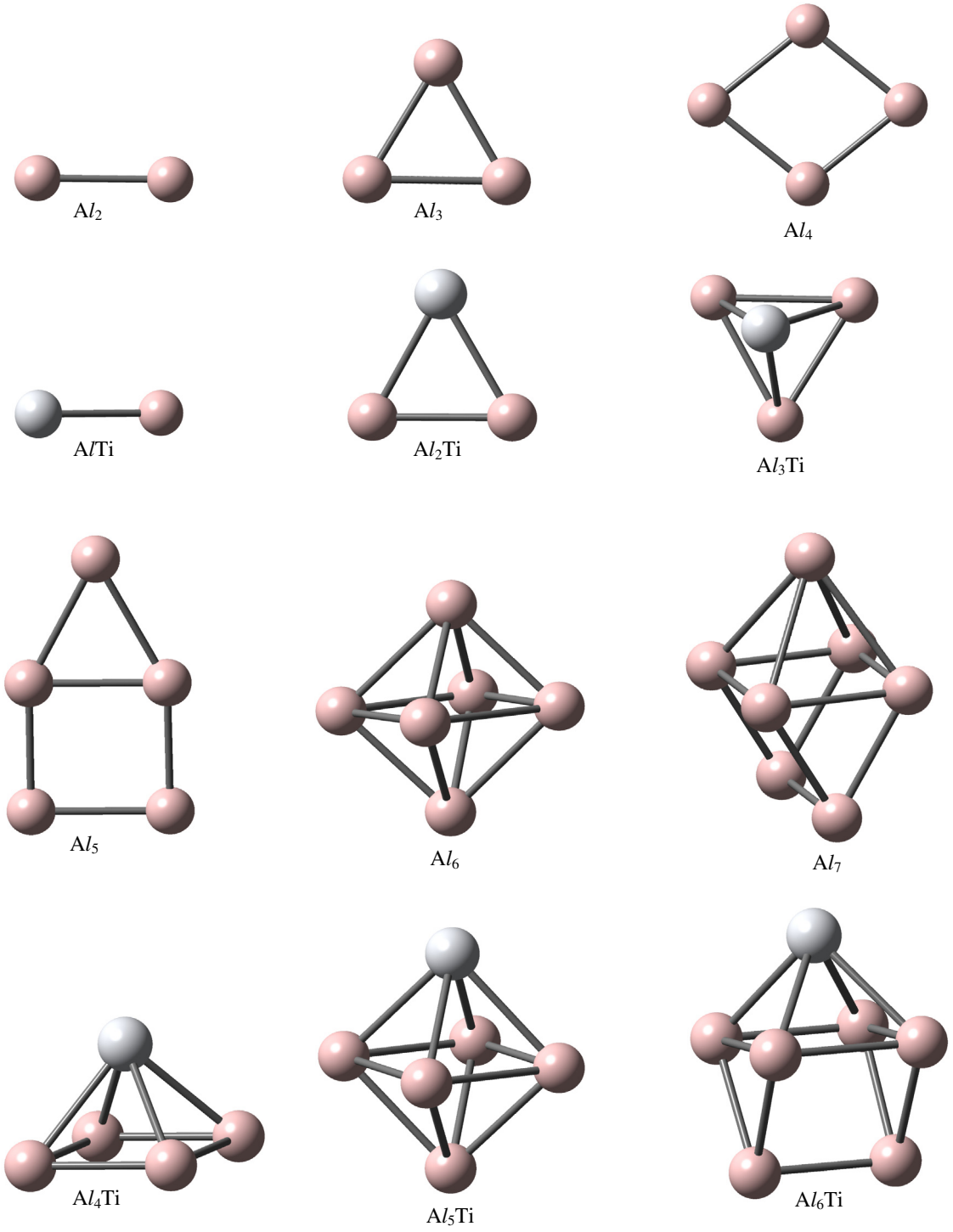

Fig. 1. Equilibrium geometries of anionic Al_n and $Al_{n-1}Ti$ ($n \leqslant 7$) type clusters.

Refs. [2–18,33–36] were verified using DFT calculations. Computationally we first searched for the global minimum of Al_n (±) and $Al_{n-1}Ti$(±) ($n \leqslant 7$) clusters using the B3LYP/6-311++G** level of theory. In total, this amounted to optimizing 190 separate geometries. Calculations are carried out without any symmetry restrictions for different starting geometries. Starting with the spin singlet configurations of even electron system and the spin doublet configuration of odd-electron system, the calculation procedure was repeated for various spin multiplicities for a given cluster size. In this work, we performed more than 500 geometric optimizations calculations. The calculations are continued until the minimum energy is reached. Frequency analysis is performed at the B3LYP/6-311++ G(d,p) level to check whether the optimized structures are transition states or true minima on the potential energy surfaces of corresponding clusters. The ground-state structures are obtained as actually equilibrium states without imaginary frequencies.

Secondly, to comparisons of these calculations to forthcoming experimental results, we was used the dunning's correlation consistent basis sets (cc-pVDZ and cc-pVTZ basis sets) for DFT

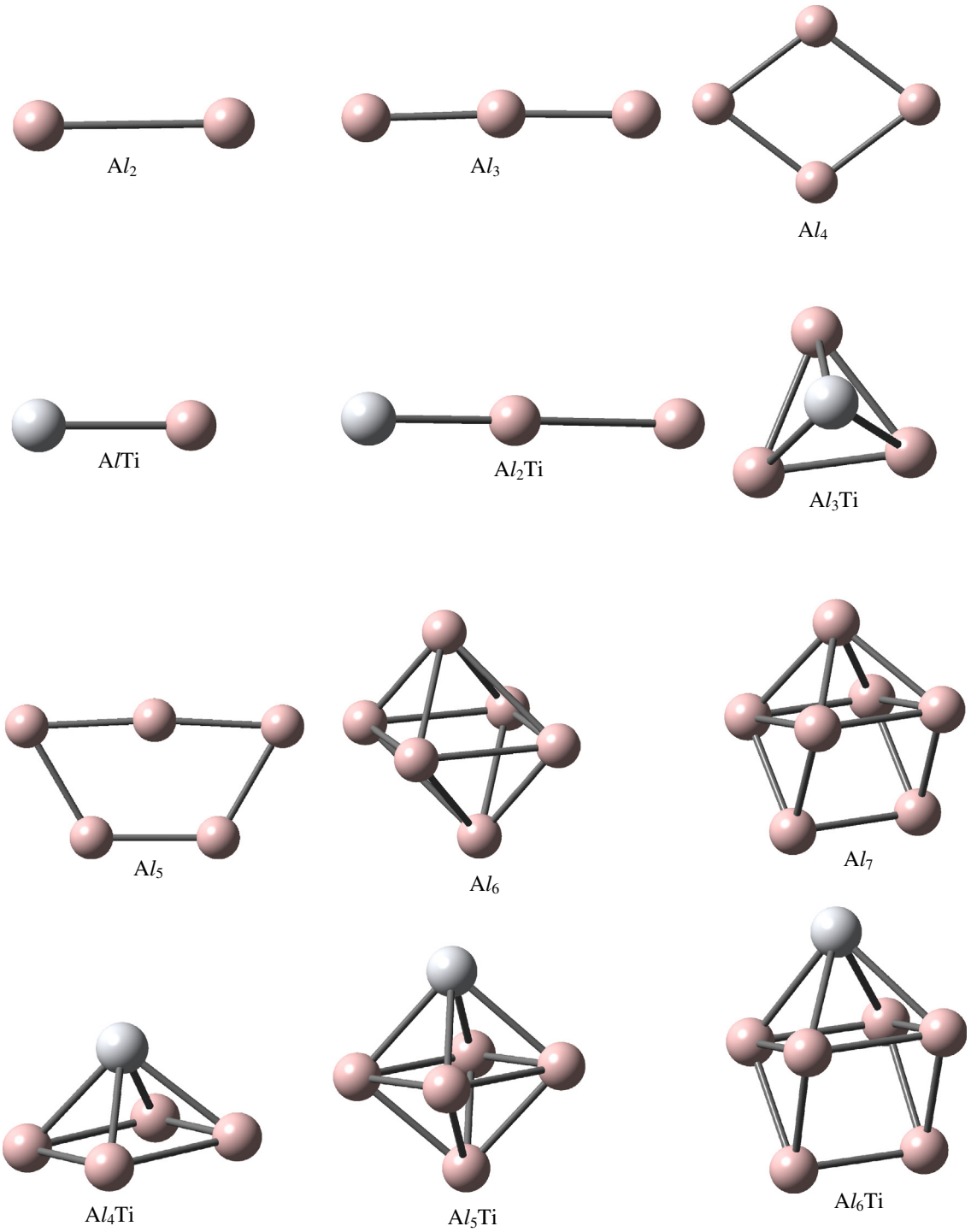

Fig. 2. Equilibrium geometries of cationic Al_n and $Al_{n-1}Ti$ ($n \leqslant 7$) type clusters.

geometry optimization calculations. For this reason, the geometries of the global minimum structures were then recalculated at B3LYP levels of theory using UB3LYP/cc-pVDZ and cc-pVTZ basis sets. In present work, vertical detachment energy, vertical and Adiabatic Electron Affinity and adiabatic ionization potentials values of Al_n (±) and $Al_{n-1}Ti$(±) ($n \leqslant 7$) isomer accurately predicts for these basis sets. Consequently, the HOMO–LUMO energy gaps, Vertical Detachment Energy, Vertical and Adiabatic Electron Affinity and Adiabatic Ionization Potentials of Al_n (±) and $Al_{n-1}Ti$(±) ($n \leqslant 7$) clusters were reported by using the UB3LYP/ 6-311++G(d,p), cc-pVDZ and cc-pVTZ level of theory in this work.

3. Results and discussion

3.1. Structures of Al_n and $Al_{n-1}Ti$ ($n \leqslant 7$) clusters

In this paper, we are concerned with the stability and properties of cationic (single positive charge) and anionic (single negative charge) clusters. Geometry optimization for all these charge states and different spin multiplicities were carried out for each of the titanium doped aluminum clusters containing 2 to 7 atoms. The lowest-energy structures of the Al_n (±) and $Al_{n-1}Ti$(±) ($n \leqslant 7$) clusters are shown in Figs. 1 and 2. All cluster naming and geometries

Table 1
Energetics of the most stable charged (anionic) Al_n and $Al_{n-1}Ti$ clusters. Multiplicity ($2S + 1$), total energy (E_t, in a.u.), relative energy (E_r, in eV).

	Clusters	2S + 1	E_t	E_r
1	AlTi	Singlet	−1091.79476615	0.729
		Triplet	−1091.80927781	0.334
		Quintet	−1091.82157480	0.000
		Septet	−1091.78236859	1.066
2	Al_2	Doublet	−484.84823117	0.611
		Quartet	−484.87071201	0.000
		Sextet	−484.75074598	3.262
3	Al_2Ti-1	Doublet	−1334.28955137	0.133
		Quartet	−1334.29445940	0.000
		Sextet	−1334.28305666	0.310
4	Al_3-2	Singlet	−727.33985108	0.000
		Triplet	−727.32985552	0.272
5	Al_3Ti-4	Singlet	−1576.75188987	0.525
		Triplet	−1576.76651589	0.127
		Quintet	−1576.77120378	0.000
		Septet	−1576.74137392	0.811
6	Al_4-2	Doublet	−969.80391602	0.000
		Quartet	−969.79863671	0.144
7	Al_4Ti-10	Doublet	−1819.24678612	0.282
		Quartet	−1819.25716180	0.000
		Sextet	−1819.24716180	0.272
8	Al_5-5	Singlet	−1212.27092443	0.000
		Triplet	−1212.23920154	0.863
9	Al_5Ti-8	Singlet	−2061.69182889	0.093
		Triplet	−2061.69524291	0.000
		Quintet	−2061.69508084	0.004
10	Al_6-6	Doublet	−1454.75066880	0.000
		Quartet	−1454.73114601	0.531
12	Al_6Ti-17	Doublet	−2304.16642393	0.826
		Quartet	−2304.19679574	0.000
		Sextet	−2304.16156228	0.958
13	Al_7-8	Singlet	−1697.22667506	0.000
		Triplet	−1697.22205119	0.126

Table 2
Energetics of the most stable charged (cationic) Al_n and $Al_{n-1}Ti$ clusters. Multiplicity ($2S + 1$), total energy (E_t, in a.u.), relative energy (E_r, in eV).

	Clusters	2S + 1	E_t	E_r
1	AlTi	Singlet	−1091.50043939	1.936
		Triplet	−1091.55414147	0.475
		Quintet	−1091.57162482	0.000
		Septet	−1091.40657283	4.488
2	Al_2	Doublet	−484.58463719	0.000
		Quartet	−484.49164046	2.529
3	Al_2Ti-2	Doublet	−1333.99421492	0.757
		Quartet	−1334.02206510	0.000
		Sextet	−1334.00164197	0.555
4	Al_3-1	Singlet	−727.04908122	0.000
		Triplet	−727.04213677	0.189
5	Al_3Ti-4	Singlet	−1576.48252392	0.272
		Triplet	−1576.49251206	0.000
		Quintet	−1576.49123314	0.035
6	Al_4-2	Doublet	−969.48817547	0.185
		Quartet	−969.49496145	0.000
		Sextet	−969.44216176	1.436
7	Al_4Ti-10	Doublet	−1818.96212675	0.060
		Quartet	−1818.96432745	0.000
		Sextet	−1818.94507687	0.523
8	Al_5-4	Singlet	−1211.95599603	0.089
		Triplet	−1211.95925344	0.000
		Quintet	−1211.94995507	0.253
9	Al_5Ti-8	Singlet	−2061.40113537	0.000
		Triplet	−2061.39639882	0.129
10	Al_6-6	Doublet	−1454.42777817	0.000
		Quartet	−1454.42040590	0.200
11	Al_6Ti-17	Doublet	−2303.90953627	0.000
		Quartet	−2303.88894890	0.560
12	Al_7-8	Singlet	−1696.94874080	0.000
		Triplet	−1696.90874165	1.088

were determined based on the previous article [37]. The optimized energies and relative energies of these clusters for various spin multiplicities of the most stable structures are given in Tables 1 and 2. The results of these optimizations are discussed in the following section.

The experimental work of Ginter et al. [38] found to have a triplet spin multiplicity for Al_2. Magnetic deflection experiments by Cox et al. [39] found the same results with Ginter et al. [38] for Aluminum dimers. Using different basis sets and different methods treatments, Bauschlicher et al. [40] found the triplet spin multiplicity to be the most stable state for Al_2. Previous work indicated that the most stable state is the triplet spin multiplicity for Al_2 ($S = 1$). For ionic cases, we found that the most stable state is the quartet ($S = 3/2$) and doublet ($S = 1/2$) spin multiplicity anionic and cationic case, respectively.

We found that the AlTi dimer has the sextet spin multiplicity for neutral case. In the present work, the results imply that the quintet spin multiplicity of AlTi dimer is the most stable state for both ionic cases.

For Al_3 clusters, there are two possible isomer models. One of these clusters is triangle geometry. Other cluster is linear structure. In the previous work [37], we found that the triangle geometry of Al_3 trimer is more stable than the linear geometry. The linear geometry energy is about 0.451 eV greater than that of the triangle geometry. In addition, the previous work indicates that the most stable form of Al_3 trimer has a doublet spin multiplicity [37]. For cationic case, energy difference between triangle and linear geometry are 0.272 eV. While triangle geometry of Al_3 is the most stable structure for cationic case, linear geometry is the most stable structure for anionic case.

For Al_2Ti clusters, one of these clusters is an isosceles triangle with doped atoms at the apex. Other clusters are linear structures. For the linear structure, there are two possible isomer models. Figs. 1 and 2 show that the Ti atom occupying the central and terminal positions. For anionic case, we determined that the lowest-energy structure for Al_2Ti is an isosceles triangle (Figs. 1 and 2) with Ti at the apex by B3LYP/6-311++G(d,p) level of theory. The present calculations indicate that the relative energy between the quartet spin multiplicity and Doublet multiplicity, Sextet multiplicity 0.133 eV and 0.310 eV by B3LYP/6-311++G(d,p) level of theory for the most stable structure. For cationic case, the present calculations indicate that an isosceles triangle with Ti at the apex is 0.004 eV lower than that of the titanium atom occupying a terminal position of linear structure. We find that the Al_2Ti-1 (sextet multiplicity) and Al_2Ti-2 (Quartet multiplicity) are the most stable structures of Al_2Ti trimer clusters. Al_2Ti-1 and Al_2Ti-2 are degenerate stable structure.

We performed structural optimizations for one-dimensional (1D) (Al_4 (a)), two-dimensional (2D) (Al_4 (b, d and)) and three-dimensional (3D) (Al_4 (c)) models of aluminum clusters. In the previous work, we determined that the rhombus geometry has the most stable structure. For cationic and anionic case, the rhombus geometry has also the most stable structure for Al_4 tetramers. While the doublet spin multiplicity of rhombus structure is the most stable for anionic case, the quartet spin multiplicity of this structure is the most stable for cationic case.

The rhombus geometry is the most stable for the pure Aluminum tetramer clusters [37]. In the Titanium doped Aluminum

Table 3
HOMO, LUMO and HOMO–LUMO Gap (E_{GAP}) energies (in eV) of the clusters studied.

Clusters		HOMO			LUMO			E_{GAP}		
		6-311++G(d.p)	cc-PVDZ	cc-PVTZ	6-311++G(d.p)	cc-PVDZ	cc-PVTZ	6-311++G(d.p)	cc-PVDZ	cc-PVTZ
Anion										
Al_2	α	0.202	0.597	0.501	2.765	3.421	3.313	2.563	2.824	2.812
	β	−1.821	−1.382	−1.474	1.932	2.535	2.406	3.753	3.918	3.880
Al_2Ti	α	−0.335	−0.076	−0.123	1.663	1.947	1.905	1.998	2.023	2.028
	β	0.050	0.216	0.160	1.342	1.513	1.483	1.291	1.298	1.323
Al_4	α	−0.653	−0.448	−0.486	1.258	1.571	1.485	1.911	2.019	1.971
	β	−0.612	−0.394	−0.453	0.696	0.938	0.904	1.308	1.332	1.357
Al_4Ti	α	−0.670	−0.588	−0.597	1.350	1.459	1.431	2.020	2.047	2.029
	β	−0.748	−0.655	−0.682	1.411	1.572	1.545	2.159	2.227	2.227
Al_6	α	−1.105	−0.983	−1.034	1.009	1.183	1.160	2.113	2.166	2.194
	β	−1.077	−0.930	−0.973	0.281	0.446	0.421	1.358	1.376	1.394
Al_6Ti	α	−0.714	−0.719	−0.708	0.561	1.254	1.227	1.275	1.974	1.935
	β	−0.263	−1.087	−1.093	0.755	1.086	1.084	1.018	2.173	2.177
AlTi	α	0.158	0.268	0.240	1.990	2.389	2.331	1.832	2.122	2.092
	β	–	–	–	–	–	–	–	–	–
Al_3	α	−0.278	0.122	0.012	1.301	1.680	1.594	1.579	1.558	1.581
	β	–	–	–	–	–	–	–	–	–
Al_3Ti	α	−0.401	−0.298	−0.323	1.479	1.656	1.623	1.880	1.954	1.946
	β	–	–	–	–	–	–	–	–	–
Al_5	α	−0.850	−0.657	−0.717	0.768	0.965	0.922	1.618	1.622	1.639
	β	–	–	–	–	–	–	–	–	–
Al_5Ti	α	−0.983	−0.936	−0.938	0.689	0.779	0.771	1.673	1.716	1.708
	β	–	–	–	–	–	–	–	–	–
Al_7	α	−0.818	−0.704	−0.718	0.658	0.704	0.775	1.476	1.408	1.493
	β	–	–	–	–	–	–	–	–	–
Cation										
Al_2	α	−9.311	−9.336	−9.315	−8.400	−7.397	−7.371	0.911	1.939	1.944
	β	−12.791	−12.758	−12.724	−8.290	−7.308	−7.262	4.501	5.451	5.462
Al_2Ti	α	−8.691	−8.673	−8.682	−6.401	−6.409	−6.408	2.290	2.264	2.274
	β	−8.468	−8.456	−8.454	−6.483	−6.488	−6.494	1.985	1.969	1.960
Al_4	α	−9.309	−9.324	−9.320	−7.489	−7.413	−7.358	1.820	1.912	1.961
	β	−10.597	−10.583	−10.520	−7.955	−7.941	−7.913	2.642	2.642	2.608
Al_4Ti	α	−9.603	−9.630	−9.605	−7.100	−7.086	−7.057	2.503	2.544	2.548
	β	−9.462	−9.418	−9.430	−7.677	−7.684	−7.663	1.785	1.734	1.766
Al_6	α	−9.275	−9.253	−9.274	−7.503	−7.448	−7.459	1.772	1.804	1.815
	β	−9.277	−9.265	−9.289	−7.849	−7.814	−7.804	1.429	1.451	1.485
Al_6Ti	α	−8.971	−8.912	−8.552	−7.199	−6.748	−6.660	1.772	2.164	1.892
	β	−8.833	−8.788	−8.775	−6.502	−7.575	−7.596	2.330	1.214	1.179
AlTi	α	−9.746	−9.606	−9.635	−6.957	−7.562	−7.551	2.789	2.044	2.084
	β	–	–	–	–	–	–	–	–	–
Al_3	α	−8.305	−9.392	−9.387	−6.827	−7.244	−7.227	1.478	2.148	2.160
	β	–	–	–	–	–	–	–	–	–
Al_3Ti	α	−9.479	−9.490	−9.523	−7.140	−6.970	−6.975	2.339	2.520	2.548
	β	–	–	–	–	–	–	–	–	–
Al_5	α	−9.225	−9.193	−9.218	−7.539	−7.543	−7.505	1.687	1.650	1.713
	β	–	–	–	–	–	–	–	–	–
Al_5Ti	α	−8.996	−9.343	−9.364	−7.458	−7.385	−7.369	1.538	1.958	1.995
	β	–	–	–	–	–	–	–	–	–
Al_7	α	−9.363	−9.365	−9.381	−6.680	−6.699	−6.651	2.683	2.666	2.730
	β	–	–	–	–	–	–	–	–	–

tetramer cluster, tetrahedral structure is the most stable geometry according to DFT calculations. We note that three Al atoms form an equilateral triangular and Ti atom caps the surface resulting in a tetrahedral configuration.

The Al_5−1 is linear structure (1D), Al_5−2 − Al_5−7 structures are planar (2D) and Al_5−8 structure is Pyramidal structure (3D). For anionic clusters containing 5 Al atoms, the most stable structure is planar the Al_5−5 geometry. For cationic case, the most stable structure is planar the Al_5−4 geometry. The present calculation results for the most stable cationic Al_5 agree with the most stable form of neutral Al_5 cluster [37]. But, anionic geometry is turned into different geometry (Al_5−5 geometry). The structure of anionic geometry results agree with the result of Fournier [41].

From energetics point of view, Al_4Ti-10 model has the lowest energy, which has pentagonal pyramide geometry. Wang et al. [22] reported that the lowest-energy structure of the Transition

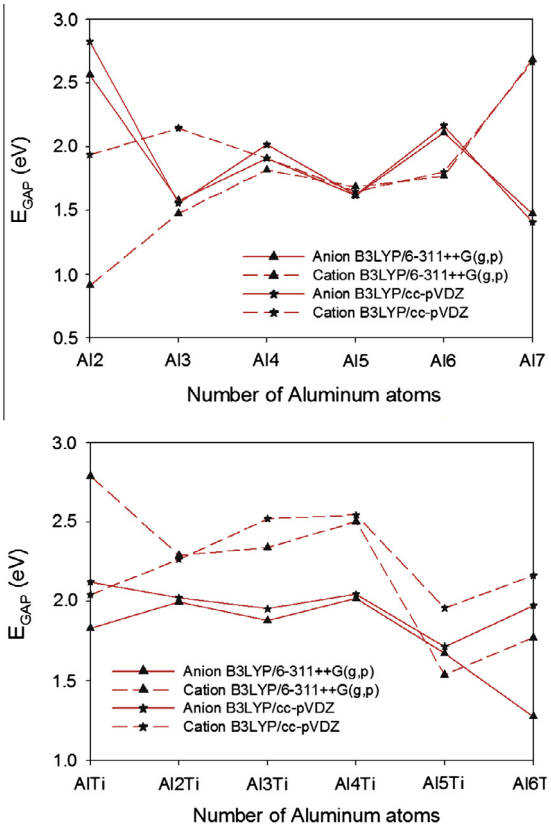

Fig. 3. Variation of HOMO–LUMO gap (E_{gap}) versus cluster size for systems with α-spin state.

Metal doped (TM: Chromium, Manganese, Iron, Cobalt and Nickel) Aluminum pentamers are pentagonal pyrimade structure. In the previous work, we note that the pentagonal pyrimade structure of Al_4Ti pentamer cluster is the most stable geometry. The present results agree with the result of our [37] and Wang [22].

The previously results show that the most stable geometry of Al_6 is the Octahedron structure. For ionic clusters containing 5 atoms, the geometry becomes three dimensional. We found that the most stable structure for (both cationic and anionic case) Al_6 is the Octahedron, as shown in Figs. 1 and 2. The present calculation results for the most stable Al_6 agree with the most stable form found by Jones [5], Petterson [6], Upton [42], etc.

According to our calculations, the lowest-energy structure for Al_5Ti is the octahedron with Ti at one apex. The Titanium impurity in the ground state structure can be look upon as the substitution apical Al atom in the ground state Al_6 hexamer clusters. The total energy of Al_5Ti is increased by 0.004 eV when the spin changes from triplet to quintet spin state.

For clusters containing seven atoms, the geometry transform into a three-dimensional motif. This clusters growth pattern is based on the octahedron of Al_6 hexamers. The ground-state structure of this cluster can be obtained by putting an atom on one face of the octahedron structure for the Al_6 cluster as shown in Figs. 1 and 2 (Al_7-8 cluster). Ahlrichs et al. [43] reported that the most stable geometry is found for Al_7 heptamers with the structure of a capped octahedron structure. The present calculation results for the most stable single charged Al_7 agree with the most stable form found by Ahlrichs et all. [43].

For cationic and ionic case, the most stable geometry of the Titanium doped Al_6 heptamers are shown in Figs. 1 and 2. Al_6Ti heptamers, which are generated from Al_7-8 is the most stable geometry. The Al_6Ti-17 cluster is generated from Al_7-8 cluster with doped Titanium atom at the apex. For previous work [37], we note

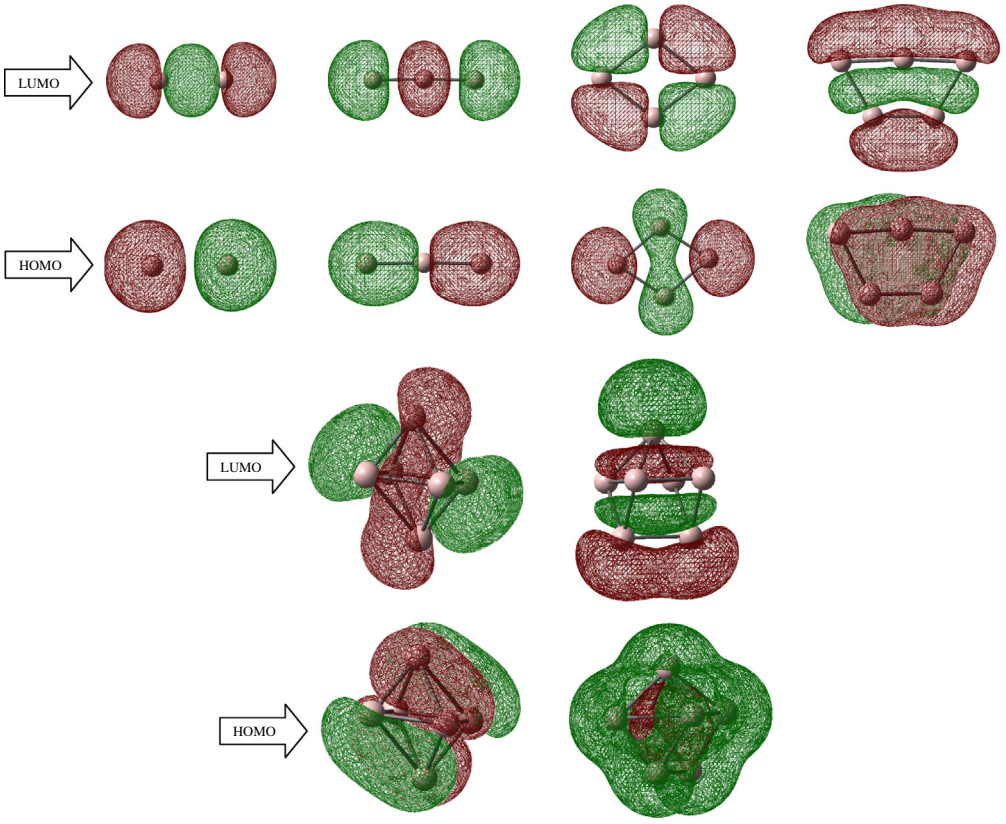

Fig. 4a. HOMO–LUMO plots of pure cationic clusters.

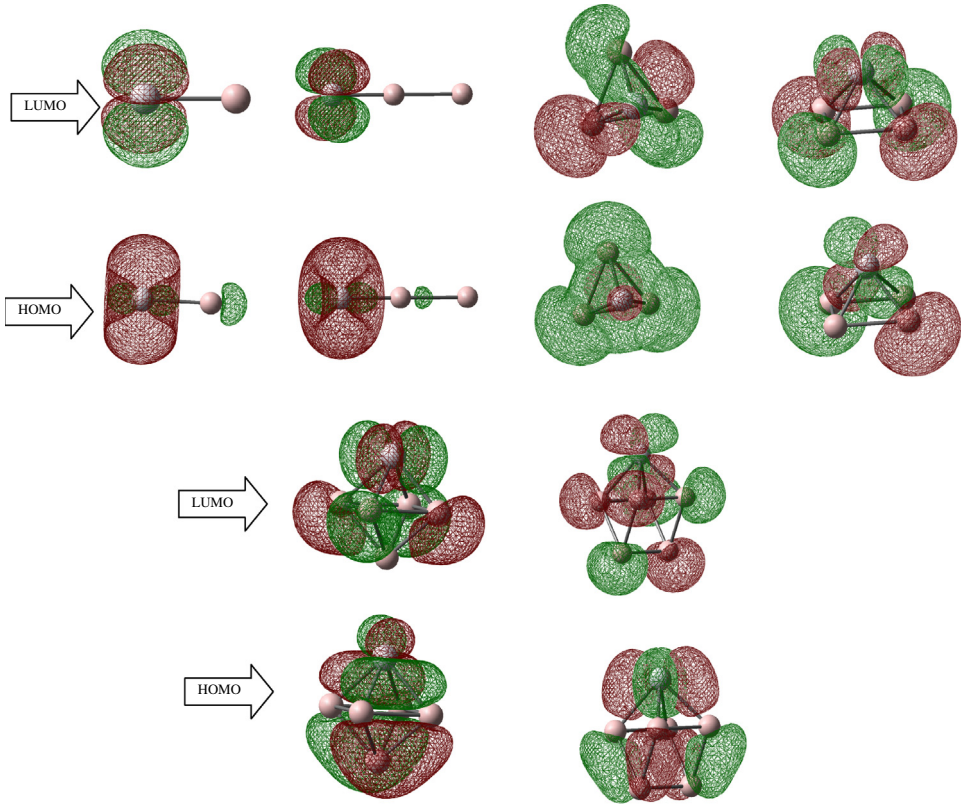

Fig. 4b. HOMO–LUMO plots of Titanium doped cationic clusters.

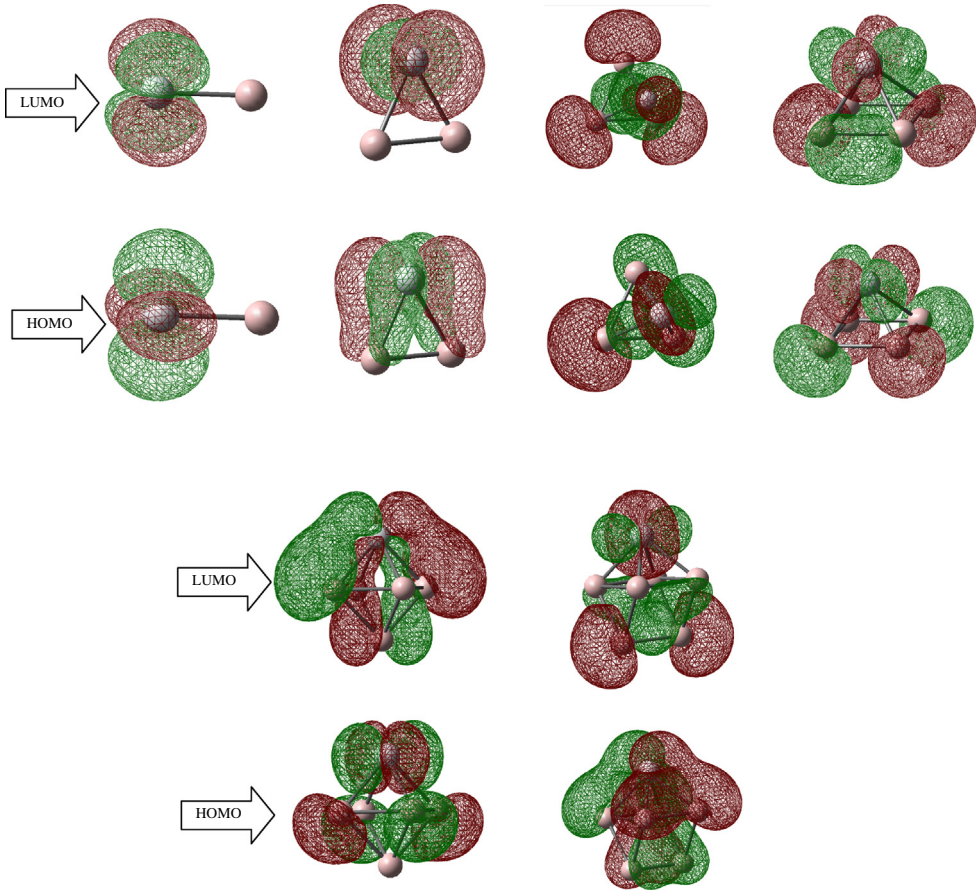

Fig. 4c. HOMO–LUMO plots of Titanium doped anionic clusters.

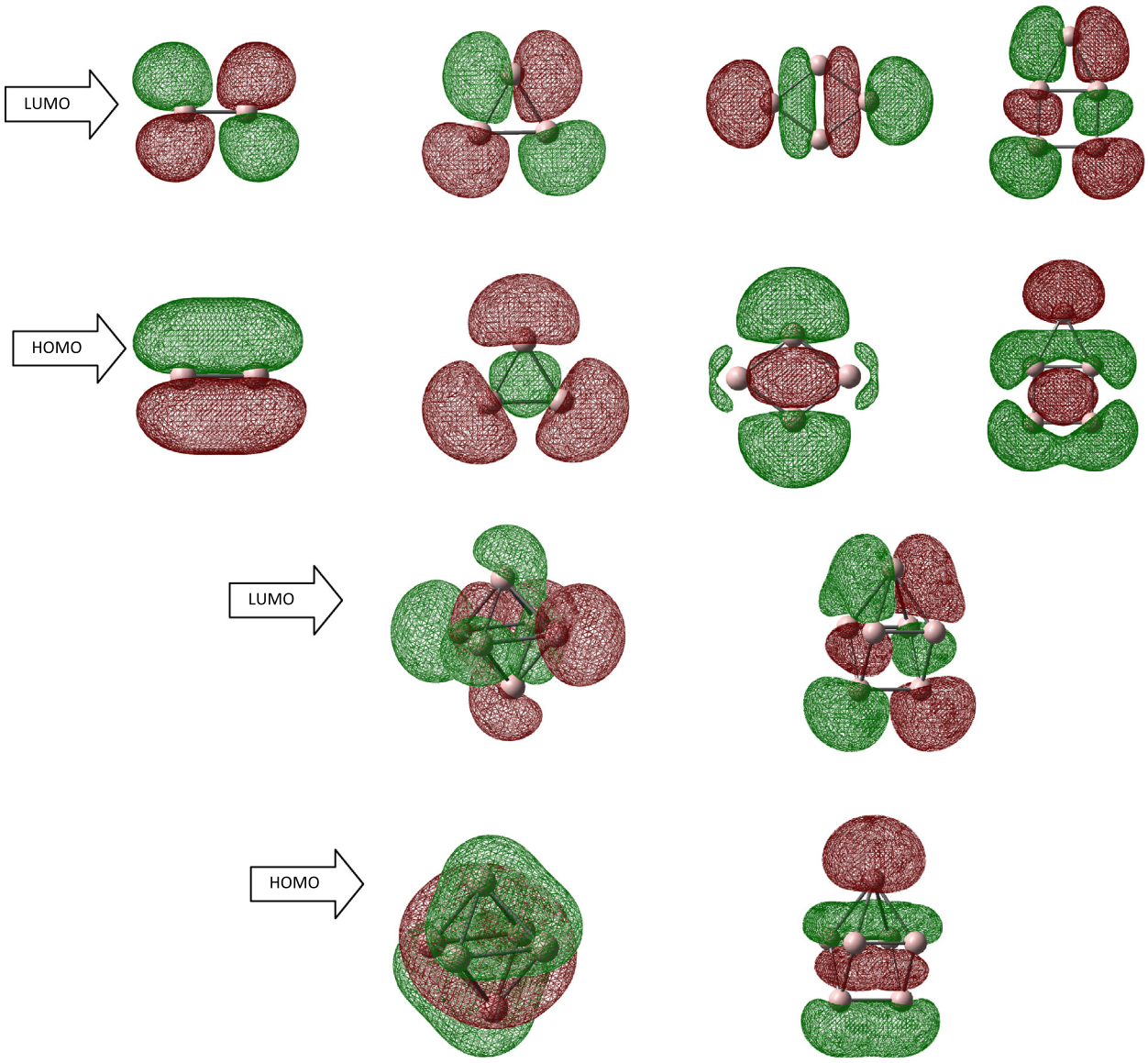

Fig. 4d. HOMO–LUMO plots of pure anionic clusters.

that this cluster is the most stable geometry. The present calculations indicate that the most stable form of Al_6Ti heptamers are not changed for neutral and ionic case.

3.2. Electronic properties

The evolution of the electronic structure can be probed by calculating the highest occupied molecular orbital (HOMO) as well as the energy gap (E_{GAP}) between HOMO and the lowest unoccupied molecular orbital (LUMO). The energy gap is a characteristic quantity of electronic structure of clusters and also a measure of stability for clusters to undergo activated chemical reactions with small molecules. Since the number of electrons in Al_3, Al_3Ti, Al_5, Al_5Ti, Al_7 and AlTi cluster are even, these clusters have only α-states; on the other hand, the remaining clusters have an odd number of electrons hence they have both α and β-states. The HOMO, LUMO, and E_g values of the systems studied are tabulated in Table 3. Variations of HOMO–LUMO gap (E_{gap}) versus cluster size are given in Fig. 3.

DFT calculations show that the HOMO–LUMO gap values of Al_n with even n are more slightly larger than those with odd n for anionic case. While the E_{GAP} value of Al_7 is the largest in cationic case, the E_{GAP} value of Al_2 is the largest in anionic case. We reported that the E_{GAP} value of neutral pure Al_2 cluster is the smaller than those of other neutral pure clusters [37]. But, the E_{GAP} value of pure Al_2 cluster is the larger than ones by adding an electron.

The HOMO will play an important role in relaxing the structure after losing an electron from a molecule. Usually, the geometries of the structure after losing an electron from its HOMO have much variation if HOMO is a bonding orbital, while the structure has no obvious difference after losing an electron from a non-bonding or weak bonding orbital. We hereby show the pictures of the HOMOs of charged Al_n and $Al_{n-1}Ti$ ($n \leqslant 7$) clusters in Figs. 4a–d in order to explore the changes of the structures after losing an electron from the HOMO of clusters.

3.3. Ionization potentials and electron affinities

Other important properties that reflect the stability of cluster are their ionization potentials (IPs) and electron affinities (EAs) [44,45]. Here, the IPs and EAs were calculated from the total

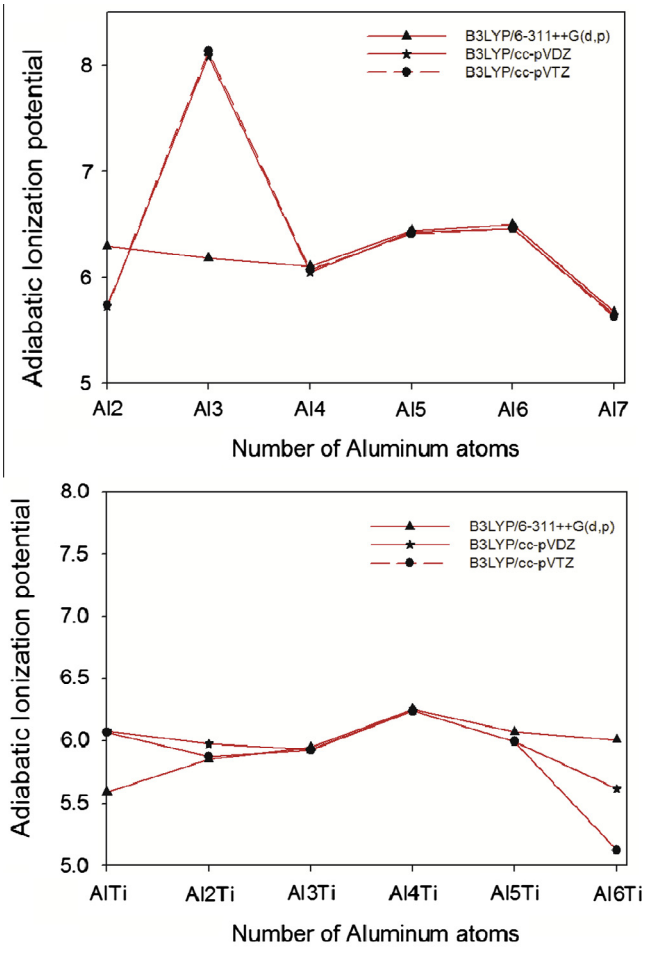

Fig. 5. Variation of ionization potential versus cluster size.

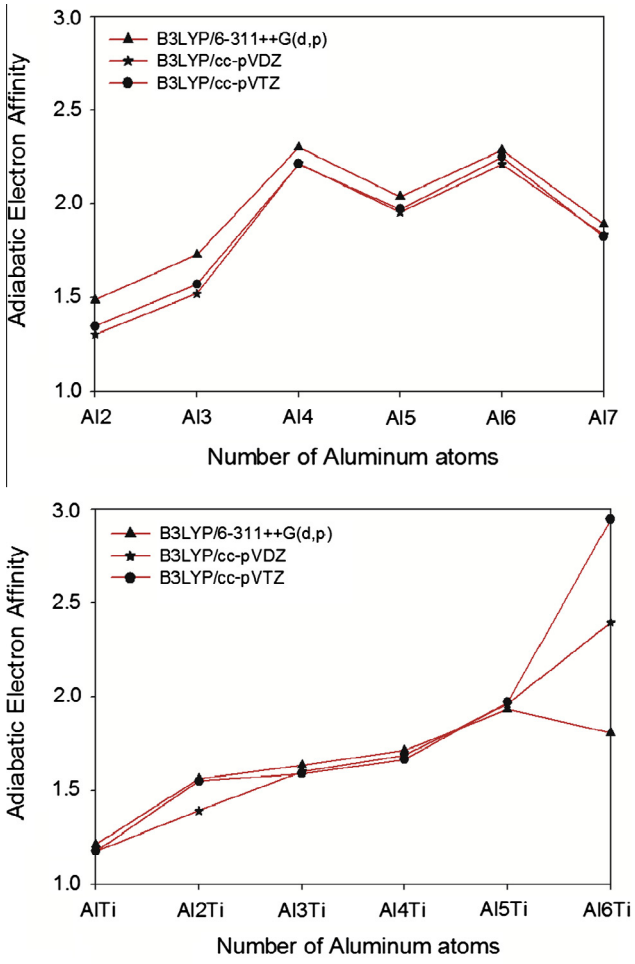

Fig. 6. Variation of Adiabatic Electron Affinity versus cluster size.

energies of the most stable the charged pure and titanium doped aluminum clusters.

$$\mathrm{IP} = E(\text{optimized cation}) - E(\text{optimized neutral}) \quad (1)$$

The ionization potential (IP) measures the energy difference between the ground state of the neutral and the ionized clusters (cationic case). If the ionized cluster has the same geometry as the ground state of the neutral, the ionization energy corresponds to the vertical ionization potential (VIP). On the other hand, the energy difference between the ground state of the cation and ground state of the neutral is referred to as the adiabatic ionization potential (AIP). Thus the vertical ionization potential is always larger than the adiabatic ionization potential and the energy difference between them is an indication of the energy gain due to structural relaxation. In this work, we evaluated the adiabatic ionization potential versus cluster size.

In Fig. 5, I present the evolution of the ionization potential with the cluster size. The calculated ionization potential using the B3LYP with 6-311++G(d,p), cc-pVDZ and cc-pVTZ basis sets are compared in Table 4. There are two important features to be noted in Fig. 5. First, the pure clusters (Al_3) with $n = 3$ show higher values for AIP. Second, for Titanium doped clusters, the AIP values have the tendency of increase until the number of Al_4Ti units in the cluster increases.

A different situation in adiabatic ionization potential of Al_3 clusters occur at B3LYP/6-311++G(d,p) level of theory. In the neutral Al_3 cluster, the Al–Al bond length was predicted at 2.789 Å [40]. Similarly, the Al-Al bond length of Al_3 clusters are predicted at 2.484 Å (B3LYP/cc-pVDZ) and 2.477 Å (B3LYP/cc-pVTZ) for cationic case. But, these bond lengths are predicted at 3.104 Å (B3LYP/6–311++G(d,p)). In a results, adiabatic ionization potential of Al_3 clusters decrease due to changing the geometry in B3LYP/6-311++G(d,p).

Table 4
Ionization potential (in eV) values of pure and titanium doped aluminum clusters.

Pure aluminum clusters				Titanium doped aluminum clusters			
Clusters	6–311++G(d.p)	cc-PVDZ	cc-PVTZ	Cluster	6–311++G(d.p)	cc-PVDZ	cc-PVTZ
Al_2	6.296	5.728	5.740	AlTi	5.589	6.080	6.080
Al_3	6.184	8.087	8.130	Al_2Ti	5.851	5.975	5.875
Al_4	6.106	6.048	6.072	Al_3Ti	5.949	5.931	5.929
Al_5	6.442	6.426	6.409	Al_4Ti	6.255	6.243	6.242
Al_6	6.499	6.462	6.461	Al_5Ti	6.071	5.992	5.995
Al_7	5.671	5.646	5.627	Al_6Ti	6.007	5.614	5.122

Table 5
Adiabatic electron affinities (in eV) values of pure and titanium doped aluminum clusters.

Pure aluminum clusters				Titanium doped aluminum clusters			
Clusters	B3LYP	B3LYP	B3LYP	Clusters	B3LYP	B3LYP	B3LYP
	6-311++G(d.p)	cc-PVDZ	cc-PVTZ		6–311++G(d.p)	cc-PVDZ	cc-PVTZ
Al_2	1.488	1.305	1.347	AlTi	1.212	1.652	1.176
Al_3	1.728	1.520	1.571	Al_2Ti	1.562	1.392	1.551
Al_4	2.301	2.215	2.213	Al_3Ti	1.634	1.600	1.591
Al_5	2.039	1.957	1.972	Al_4Ti	1.713	1.688	1.667
Al_6	2.288	2.211	2.250	Al_5Ti	1.932	1.418	1.971
Al_7	1.892	1.834	1.825	Al_6Ti	1.809	2.396	2.947

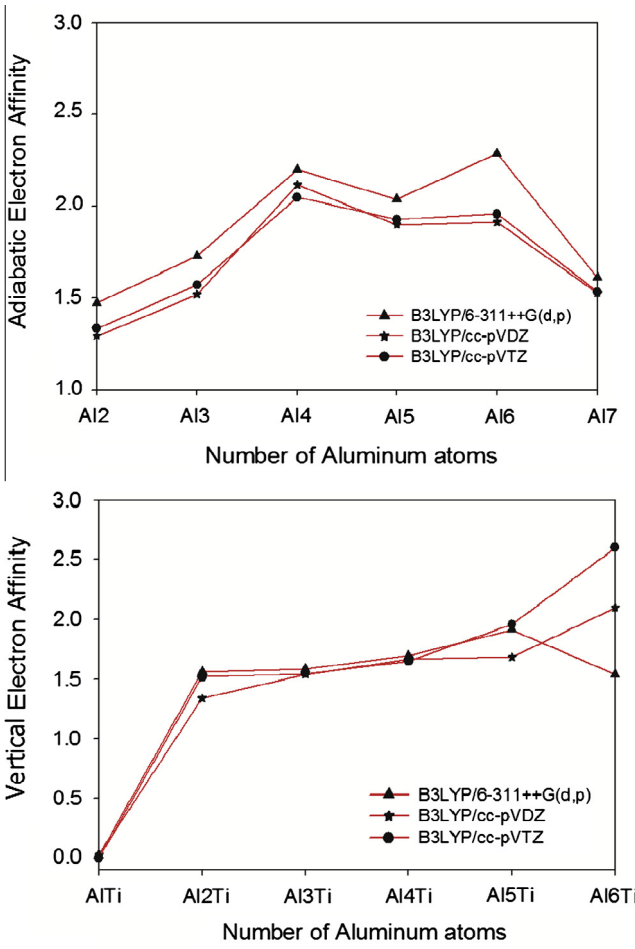

Fig. 7. Variation of vertical electron affinity versus cluster size.

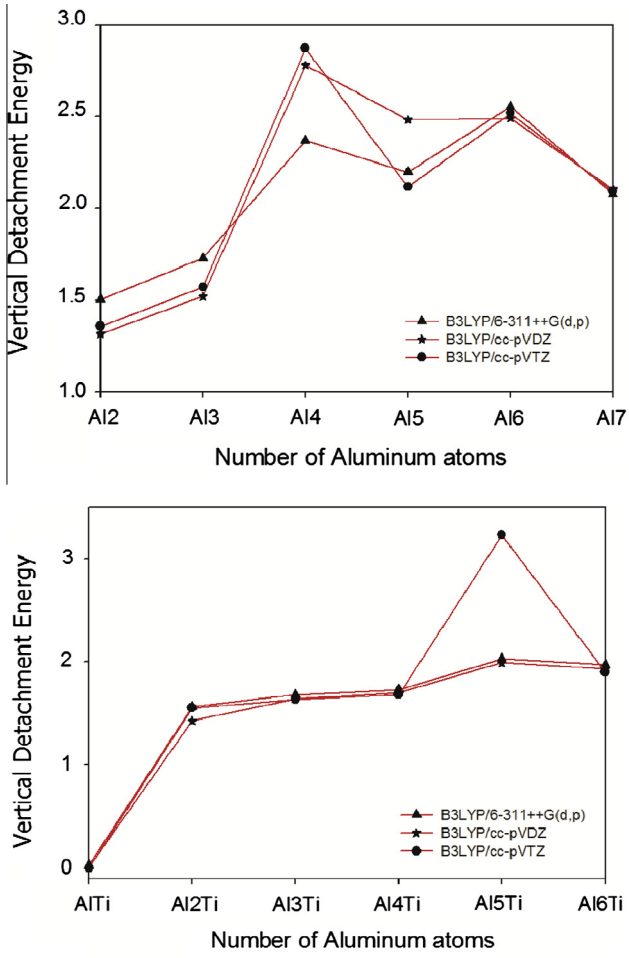

Fig. 8. Variation of Vertical Detachment Energy versus cluster size.

Table 6
Vertical electron affinity (in eV) values of pure and titanium doped aluminum clusters.

Pure aluminum clusters				Titanium doped aluminum clusters			
Clusters	B3LYP	B3LYP	B3LYP	Clusters	B3LYP	B3LYP	B3LYP
	6–311++G(d.p)	cc-PVDZ	cc-PVTZ		6–311++G(d.p)	cc-PVDZ	cc-PVTZ
Al_2	1.473	1.294	1.335	AlTi	0.027	0.024	1.176
Al_4	1.728	1.520	1.571	Al_2Ti	1.561	1.339	1.519
Al_6	2.200	2.117	2.048	Al_3Ti	1.585	1.541	1.544
Al_3	2.039	1.900	1.928	Al_4Ti	1.696	1.665	1.652
Al_5	2.288	1.912	1.957	Al_5Ti	1.915	1.683	1.959
Al_7	1.610	1.525	1.533	Al_6Ti	1.539	2.098	2.603

Table 7
Vertical detachment energy (in eV) values of pure and titanium doped aluminum clusters.

Pure aluminum clusters				Titanium doped aluminum clusters			
Clusters	B3LYP	B3LYP	B3LYP	Clusters	B3LYP	B3LYP	B3LYP
	6–311++G(d.p)	cc-PVDZ	cc-PVTZ		6–311++G(d.p)	cc-PVDZ	cc-PVTZ
Al_2	1.502	1.316	1.357	AlTi	0.026	0.002	0.000
Al_4	1.728	1.520	1.571	Al_2Ti	1.562	1.427	1.553
Al_6	2.370	2.781	2.872	Al_3Ti	1.677	1.642	1.632
Al_3	2.198	2.481	2.117	Al_4Ti	1.729	1.701	1.681
Al_5	2.553	2.490	2.518	Al_5Ti	2.028	1.990	3.230
Al_7	2.076	2.103	2.092	Al_6Ti	1.971	1.930	1.901

Electron affinity is the energy gained when an electron is added to the isolated atom. Adiabatic values for the electron affinity (EA_{ad}) for the lowest energy isomers of the charged pure and titanium doped aluminum clusters are computed in this study. The Adiabatic Electron Affinity (EA_{ad}) is the difference in the total energy between the ground state of the anion and the neutral cluster.

$$EA_{ad} = E(\text{optimized neutral}) - E(\text{optimized anion}) \quad (2)$$

In Fig. 6, I present the evolution of the adiabatic electron affinities with the cluster size. The calculated adiabatic electron affinities using the B3LYP with 6-311++G(d,p), cc-pVDZ and cc-pVTZ basis sets are compared in Table 5.

As seen in Fig. 6, the pure clusters with $n = 4$ and 6 show higher values for Adiabatic Electron Affinity. For Titanium doped clusters, the Adiabatic Electron Affinity values have the tendency of increase. But, Adiabatic Electron Affinity values of Al_6Ti clusters, especially B3LYP/cc-pVDZ and cc-pVTZ calculations, quickly increasing due to changing the geometry.

The vertical electron affinity (EA_{vert}) is the difference in the energy between the ground state of the anion and the energy of the neutral cluster having the anionic geometry.

$$EA_{vert} = E(\text{optimized neutral}) - E(\text{anion at optimized neutral geometry}) \quad (3)$$

In Fig. 7, I present the evolution of the vertical electron affinities with the cluster size. The calculated vertical electron affinities using the B3LYP with 6-311++G(d,p), cc-pVDZ and cc-pVTZ basis sets are compared in Table 6. In the vertical electron affinity, the same trends as observed previously for adiabatic electron affinities.

The vertical detachment energy (VDE) has also been computed, defined as the energy difference between the neutral and anionic clusters with both at the neutral cluster optimized geometry [46]. It's the energy necessary to remove an electron from the anionic cluster without changing its geometry.

$$VDE = E(\text{neutral at optimized anion geometry}) - E(\text{optimized anion}) \quad (4)$$

In Fig. 8, I present the evolution of the vertical detachment energies with the cluster size. The calculated vertical detachment energies using the B3LYP with 6-311++G(d,p), cc-pVDZ and cc-pVTZ basis sets are compared in Table 7. We determine the dependence of VDE with respect to the number of aluminum atoms

4. Conclusion

The geometries, stabilities, electronic properties, electron affinities and ionization potential of a series Charged Titanium doped Aluminum nanoclusters have been systematically investigated by Density Functional Theory calculations s at the B3LYP level. The most stable forms found for all clusters are compared with results reported by previously Authors. Vertical Detachment Energies (VDE) are obtained for all the Al_nTi-species. VDE values of Al_nTi-($n = 1-6$) are determined to be 0–3 eV region. The VDE of Al_4 cluster has the larger value. For Titanium doped clusters, the VDE of the Al_5Ti cluster has the larger value. The findings have useful implications in future investigations of phenomenon caused by the presence of Titanium doped Aluminum clusters for technological alloy system.

Acknowledgements

Y. Erdogdu would like to thank Ahi Evran University Research Fund for its financial support. Project No. FEN.4003.12.013. Computing resources used in this work were provided by the National Center for High Performance Computing of Turkey (UYBHM).

References

[1] S. Erkoc, B. Gunes, P. Gunes, Int. J. Mod. Phys. C 11 (2000) 1013.
[2] A.E. Kuznetsov, A.I. Boldyrev, H.J. Zhai, X. Li, L.S. Wang, J. Am. Chem. Soc. 124 (2002) 11791.
[3] B.K. Rao, P. Jena, J. Chem. Phys. 111 (1999) 1890.
[4] J. Akola, H. Hakkinen, M. Manninen, Phys. Rev. B 58 (1998) 3601.
[5] R.O. Jones, Phys. Rev. Lett. 67 (1991) 224; R.O. Jones, J. Chem. Phys. 99 (1993) 1194.
[6] L.G.M. Petterson, C.W. Bauschlicher Jr, J. Chem. Phys. 87 (1987) 2205.
[7] R.E. Leuchtner, A.C. Harms, A.W. Castleman Jr, J. Chem. Phys. 94 (1991) 1093.
[8] G. Gantefor, K.H. Meiwes-Broer, H.O. Lutz, Phys. Rev. A 37 (1988) 2716.
[9] W.A. Saunders, P. Fayet, L. Woste, Phys. Rev. A 39 (1989) 4400.
[10] L. Hanley, S.A. Ruatta, S.L. Anderson, J. Chem. Phys. 87 (1987) 260.
[11] M.F. Jarrold, J.E. Bower, J.S. Kraus, J. Chem. Phys. 86 (1987) 3876.
[12] M.D. Deshpande, D.G. Kanhere, I. Vasiliev, R.M. Martin, Phys. Rev. B 68 (2003) 035428.
[13] X. Li, H. Wu, X.B. Wang, L.S. Wang, Phys. Rev. Lett. 81 (1998) 1909.
[14] L.G.M. Pettersson, C.W. Bauschlicher Jr, T. Halicioglu, J. Chem. Phys. 87 (1987) 2205.
[15] O. Dolgunicheva, V.G. Zakrzewski, J.V. Ortiz, J. Chem. Phys. 111 (1999) 10762.
[16] B.K. Rao, P. Jena, J. Chem. Phys. 115 (2001) 778.
[17] L. Guo, H. Wu, J. Nanopart. Res. 10 (2008) 341.
[18] X.J. Ren, B.X. Li, Physica B 405 (2010) 2344.
[19] X.G. Gong, Phys. Rev. B 56 (1997) 1091.
[20] X.G. Gong, V. Kumar, Phys. Rev. Lett. 70 (1993) 2078.
[21] V. Kumar, V. Sundararjan, Phys. Rev. B 57 (1998) 4939.
[22] M. Wang, X. Huang, Z. Du, Y. Li, Chem. Phys. Lett. 480 (2009) 258.
[23] W.M. Sun, Y. Li, D. Wu, Z.R. Li, Phys. Chem. Chem. Phys. 14 (2012) 16467.
[24] X. Li, L.S. Wang, Phys. Rev. B 65 (2002) 153404.
[25] D.J. Henry, I. Yarovsky, J. Phys. Chem. A 113 (11) (2009) 2565–2571.
[26] D.J. Henry, P. Szarek, K. Hirai, K. Ichikawa, A. Tachibana, I. Yarovsky, J. Phys. Chem. C 115 (5) (2011) 1714–1723.
[27] O.P. Charkin, N.M. Klimenko, D.O. Charkin, A.M. Mebel, Russ. J. Inorg. Chem. 51 (2006) 599–607.
[28] V.K. Kochnev, O.P. Charkin, N.M. Klimenko, Russ. J. Inorg. Chem. 54 (2009) 1114–1126.
[29] V.K. Kochnev, O.P. Charkin, N.M. Klimenko, Russ. J. Inorg. Chem. 55 (2010) 65–74.
[30] A.D. Becke, J. Chem. Phys. 98 (1993) 5648.
[31] C. Lee, W. Yang, R.G. Parr, Phys. Rev. B 37 (1988) 785.
[32] M.J. Frisch, G.W. Trucks, H.B. Schlegel, G.E. Scuseria, M.A. Robb, J.R. Cheeseman, G. Scalmani, V. Barone, B. Mennucci, G.A. Petersson, H. Nakatsuji, M. Caricato, X. Li, H. P. Hratchian, A.F. Izmaylov, J. Bloino, G. Zheng, J.L. Sonnenberg, M. Hada, M. Ehara, K. Toyota, R. Fukuda, J. Hasegawa, M. Ishida, T. Nakajima, Y. Honda, O. Kitao, H. Nakai, T. Vreven, J. A. Montgomery Jr., J. E. Peralta, F. Ogliaro, M. Bearpark, J.J. Heyd, E. Brothers, K.N. Kudin, V.N. Staroverov, R. Kobayashi, J. Normand, K. Raghavachari, A. Rendell, J.C. Burant, S.S. Iyengar, J. Tomasi, M. Cossi, N. Rega, J.M. Millam, M. Klene, J.E. Knox, J.B. Cross, V. Bakken,

C. Adamo, J. Jaramillo, R. Gomperts, R.E. Stratmann, O. Yazyev, A.J. Austin, R. Cammi, C. Pomelli, J.W. Ochterski, R.L. Martin, K. Morokuma, V.G. Zakrzewski, G.A. Voth, P. Salvador, J.J. Dannenberg, S. Dapprich, A.D. Daniels, O. Farkas, J.B. Foresman, J.V. Ortiz, J. Cioslowski, and D.J. Fox, Gaussian 09, Revision A.02, Gaussian, Inc., Wallingford CT, 2009.
[33] V. Kumar, S. Bhattacharjee, Y. Kawazoe, Phys. Rev. B 61 (2000) 8541.
[34] Ş. Erkoc, Phys. Status Solidi B 152 (1989) 447.
[35] Ş. Erkoc, S. Katircioglu, Phys. Status Solidi B 152 (1989) 37.
[36] Z.El-Bayyari¸S. Erkoc, Phys. Status Solidi B 170 (1992) 103.
[37] Y. Erdogdu, Ş. Erkoç, J. Comput. Theor. Nanosci. 9 (2012) 837.
[38] D.S. Ginter, M.L. Ginter, K.K. Innes, Astrophys. J. 139 (1963) 365.
[39] D.M. Cox, G.J. Trevor, R.L. Whetten, E.A. Rohlfing, A. Kaldor, J. Chem. Phys. 84 (1986) 4651.
[40] C.W. Bauschlicher, H. Partridge, S.R. Langoff, P.R. Taylor, S.P. Walch, J. Chem. Phys. 86 (1987) 7007.
[41] R. Fournier, J. Chem. Theory Comput. 3 (2007) 921.
[42] [a] T.H. Upton, Phys. Rev. Lett. 56 (1986) 2168;
, J. Chem. Phys. 86 (1987) 7054.
[43] R. Ahlrichs, S.D. Elliott, Phys. Chem. Chem. Phys. 1 (1999) 13.
[44] A. Gao, G. Li, Y. Chang, H. Chen, Q.S. Li, J. Mol. Struct. Teochem. 961 (2010) 88.
[45] W. Xu, W. Bai, J. Mol. Struct. Teochem. 854 (2008) 89–105.
[46] J.C. Rienstra-Kiracofe, G.S. Tschumper, H.F. Schaefer III, Chem. Rev. 102 (2002) 231.